THE ASTROPHYSICAL JOURNAL, 446:244–249, 1995 June 10

CS(2–1) EMISSION FROM DENSE GAS IN THE BIPOLAR OUTFLOW OF CRL 618

ARSEN R. HAJIAN,[1] J. A. PHILLIPS,[2] AND YERVANT TERZIAN[1]
Received 1994 September 2; accepted 1994 December 20

ABSTRACT

We have imaged the protoplanetary nebula CRL 618 in the CS(2–1) line at 98 GHz using the Owens Valley Radio Observatory millimeter interferometer with a synthesized beam of $\sim 2''.5$. For the first time, we have resolved the molecular core of CRL 618: the gas at the systemic velocity of the nebula is distributed like a cross, concentrated along two perpendicular linear structures. We have also detected emission out to the ends of the observing bandpass, which is at ± 170 km s^{-1}. The high-velocity gas participates in a bipolar outflow, showing marked displacement with respect to the central source, with the redshifted gas generally to the west and the blueshifted gas to the east of the H II region. The spectrum of the CS line reveals a deep absorption feature that we have partially resolved.

Subject headings: ISM: jets and outflows — ISM: kinematics and dynamics — planetary nebula: individual (CRL 618) — radio lines: ISM

1. INTRODUCTION

The protoplanetary nebula CRL 618 is at an evolutionary stage midway between OH/IR stars, which have thick and mostly neutral outflowing envelopes, and planetary nebulae, which have fully detached ionized envelopes (Kwok 1986). CRL 618 is evolving toward a planetary nebula at a rapid pace. At centimeter wavelengths, the expanding H II region has been observed by Kwok & Feldman (1981), who computed a twofold brightness increase between 1977 and 1980. The optical brightening timescale is ~ 30 yr (Gottlieb & Liller 1976), and since the optically emitting lobes are expanding at a speed of ~ 20 km s^{-1} and the ionization front at ~ 220–330 km s^{-1} (Kwok & Feldman 1981), the young age of CRL 618 is confirmed by both observations. Furthermore, based on a distance of 1.5 kpc (Lo & Bechis 1976), the luminosity of CRL 618 is about $2 \times 10^4 D^2_{1.5\,\mathrm{kpc}}\, L_\odot$, which is similar to the luminosity of a typical, bright planetary nebula (PN) (Kleinmann et al. 1978). CRL 618 also emits a rich optical spectrum dominated by atomic emission lines which overlay a reflected stellar continuum (Trammell, Dinerstein, & Goodrich 1993; Schmidt & Cohen 1981; Kelly, Latter, & Reike 1992) and an infrared and submillimeter continuum spectrum characterized by thermal emission produced by warm dust at temperatures of order 150–250 K (Westbrook et al. 1975; Soptka et al. 1985; Kwok, Hrivnak, & Milone 1986), as well as numerous molecular emission lines emanating from the large molecular sheath surrounding the dusty condensation around CRL 618. There have been single-dish observations of several molecules from CRL 618; these include CO, HCN, SiO, C_2H, C_3N, and HCO^+ (Lo & Bechis 1976; Bujarrabal et al. 1988; Bachiller et al. 1988; Cernicharo et al. 1989; Martin-Pintado & Bachiller 1992; Deguichi, Claussen, & Goldsmith 1986). There are only a few interferometric maps which resolve the nebula spatially. The three which are known to us are the HCN observations by Neri et al. (1992), the ^{12}CO maps by Shibata et al. (1993), and the ^{13}CO results of Yamamura et al. (1994), all of which achieved synthesized beams of $\approx 3''$–$5''$.

Despite the simplicity of the pointlike $\lambda 6$ cm emission mapped by Kwok & Bignell (1984), the physical morphology of all material around CRL 618 is not arranged in the shape of a smooth, spherical nebula. Rather, the optical emission is concentrated in two lobes that are roughly oriented in the east–west direction separated by $\approx 7''$. A pointlike infrared source coincides with the 22 GHz VLA position which is midway between the optical lobes (Westbrook et al. 1975). Furthermore, high-resolution molecular line maps show that some molecules participate in the bipolar flow of the optically emitting lobes. Large emission wings are seen in the spectra of several molecular species, especially the ~ 200 km s^{-1} outflow observed in the CO (Cernicharo et al. 1989; Gammie et al. 1989) and HCN lines (Neri et al. 1992).

In this paper, we report observations of CRL 618 in the millimeter continuum and at the CS(2–1) transition at 98 GHz. Most previous studies of CRL 618 have concentrated on molecular lines such as CO, which trace low-density, low-excitation gas. The CS(2–1) gas efficiently radiates in a high-density environment and is a useful probe of conditions in the dense inner region of the nebula and in the high-velocity outflow. We review the observations in § 2, present the results and discussion in § 3, and conclude with a brief summary in § 4.

2. OBSERVATIONS

We observed CRL 618 in the CS(2–1) line and the $\lambda 3.1$ mm continuum using five independent configurations of the Owens Valley Radio Observatory (OVRO) millimeter interferometer. During the period of observation, 1991 November–1992 February, the interferometer consisted of three 10.4 m dishes with cryogenically cooled SIS receivers. The total integration time for CRL 618 was 36 hr, and the average single-sideband system temperature was 320 K. The phase center of the map was located at $\alpha(1950) = 04^h39^m34^s.0$, $\delta(1950) = +36°01'16''$.

The spectra line data were obtained with a digital correlator (Padin et al. 1993). A 128 MHz band with 64 independent frequency channels was centered on the CS(2–1) transition frequency at 97.98 GHz (lower sideband) and Doppler-shifted to an LSR velocity of -25 km s^{-1}. We also recorded the upper sideband spectrum at 100.98 GHz. Continuum data at the same frequencies was obtained using a wideband analog cor-

[1] Department of Astronomy and National Astronomy and Ionosphere Center Cornell University, Ithaca, NY 14853.
[2] Owens Valley Radio Observatory, Caltech 105-24, Pasadena, CA 91125.

relator with an effective bandwidth of 350 MHz. The observations of CRL 618 were interleaved every 30 minutes with a nearby point source, 3C 84 ($S_{98\,GHz} = 7.0$ Jy), to monitor the phase behavior of the array. We also used 3C 84 as a bandpass calibrator. The absolute flux scale was determined from observations of Uranus, Neptune, and 3C 273.

We used software specific to the Owens Valley millimeter array for amplitude and phase calibration of the raw line and continuum data (Scoville et al. 1993) and made images using AIPS. Uniform weighting gave a 2".7 × 2".2 CLEAN beam at position angle −5°.5. The maps have not been corrected for the response of the primary beam, which is ~1′, since the detected gas is within 10″ of the phase center (see § 3.2).

3. RESULTS AND DISCUSSION

3.1. $\lambda = 3.1$ mm *Continuum*

The gigahertz frequency continuum spectrum of CRL 618 is dominated by thermal emission from the nebular gas, and some small contribution from nebular dust. A straightforward extrapolation of the measured continuum fluxes near 100 GHz gives a spectral index $S_\nu \propto \nu^\alpha$ where $1.2 \leq \alpha \leq 0.9$ (Knapp, Sandell, & Robson 1993; Shibata et al. 1994), indicating a significant optical depth. If we had used the upper sideband to estimate the continuum flux at 98 GHz, we would have introduced an extra source of error at the ~5% level. Thus, in order to image the continuum source, we chose a more conservative approach: we mapped and CLEANed five line-free channels near the edge of the spectrometer band (the velocity range is −192.4 to −161.8 km s^{-1}). The continuum image showed an unresolved point source with flux density 1.43 Jy. The location of the peak of the continuum emission is consistent with the Very Large Array (VLA) position of the H II region (Kwok & Bignell 1984). The detected flux is consistent with continuum flux determinations by Knapp et al. (1993), Shibata et al. (1994), and Yamamura et al. (1994).

3.2. CS(2–1) *Line Emission*

In order to retrieve the spectral line information from the data, CLEAN components from the point source were Fourier transformed (see § 3.1), then subtracted from the total UV data set. The data were mapped and CLEANed using AIPS, resulting in 64 channels of data with a velocity resolution of 6.12 km s^{-1}. In Figure 1, we show the maps of the CS(2–1) line emission as a function of velocity after subtracting the −21.5 km s^{-1} systemic velocity for CRL 618 to account for the velocity of the central star relative to the Sun.

Figure 2 shows the spectrum of CRL 618 averaged over a 5″ box at the center of the map. The profile has wide line wings that extend to the edge of the observing bandpass. In order to verify the reality of the high-velocity wings it is important to be certain that the passband calibration is accurate. The passband shape of the OVRO interferometer varies at the 5% level on timescales of hours. To remove these fluctuations and to obtain a high signal-to-noise passband calibration, we observed the bright quasar 3C 84 every 30 minutes throughout the track. We applied the 3C 84 passband calibration to the upper sideband and to the lower sideband spectrum. The upper sideband spectrum at 101 GHz was flat, confirming the integrity of our calibration procedure, but the lower sideband spectrum showed broad wings extending to the edge of the passband. We believe that the wings are real because of our careful passband calibration procedure and because the high-velocity emission is offset from the phase center of the synthesis map, with red emission toward the west-northwest and blue toward east-southeast. We note that Neri et al. (1992) have also observed similar high-velocity emission in the HCN line, which has a critical density close to that of the CS(2–1) line, and whose spectral profile is similar to the CS spectrum.

The line profile also has a strong P Cygni absorption feature for $-21.1 < v < -8.9$ km s^{-1} and with optical depth $\tau = 0.054$. Similar absorption features are also seen in CO (Cernicharo et al. 1989) and HCN (Neri et al. 1992) from CRL 618. The absorption feature is caused by the presence of low-density, cool gas absorbing CS line and continuum radiation which was emitted by high-density gas closer to the star (Young et al. 1992). Low-density CS gas normally would not radiate significant line radiation and would be thus ordinarily undetectable in emission. However, the cool gas is responsible for absorbing CS and continuum photons, and it is this thus observed. The width of the absorption line and the sharpness of the blue absorption edge can constrain models of the turbulent and thermal energies in the low-velocity gas comprising the outer parts of the CS envelope (Young et al. 1992), but the linewidth is narrow and only partially resolved by our data. However, since the linewidth is ≤5 km s^{-1} and the maximum velocity in the low-velocity component of the line profile is about ≈20 km s^{-1}, we can conclude that the internal turbulence in the expanding molecular cocoon is small. As a result, we can approximate the outflow as having a single expansion velocity.

The line maps in Figure 1 suggest a bipolar morphology, as the channels adjacent to the rest velocity show displaced emission centers. In order to confirm this notion, we have created a blue map by integrating the flux (with respect to velocity) for $-168.0 < v < -8.9$ km s^{-1}, a green map (unshifted with respect to the line centroid) for $-8.9 < v < +9.5$ km s^{-1}, a red map for $+9.5 < v < +168.5$ km s^{-1}, and finally, a total intensity map integrated over the entire passband. Emission from medium and high-velocity material at low surface brightness as well as the double bipolarity of the nebula is evident from these integrated maps, which are shown in Figures 3*a*–3*d*. The centers of the two CS lobes are separated by 3″ and are oriented in the direction of the optical lobes. Our observations are consistent with the model of Carsenty & Solf (1982), who describe gas outflowing along an axis inclined 45° to the line of sight, with the blueshifted material to the east and the redshifted material to the west. In addition, there is a small blob in the southwest corner of the redshifted map (Fig. 3*c*) that is coincident with the southwest elongation in the total intensity map (see below).

The velocity-integrated emission over the whole bandpass ($-168.0 < v < +168.5$ km s^{-1}) is shown in Figure 3*d*. Integrated over solid angle, the total flux in the CS line (corrected for the absorption feature) is 28.52 Jy km s^{-1}. The only other published observation of the CS(2–1) line from CRL 618 is a single-dish spectrum published by Bujarrabal et al. (1988). There were no lines in their spectrum above a 2 σ noise level which is larger than our detected peak antenna temperature when corrected for the differences in the OVRO and IRAM synthesized beams. We converted the velocity-integrated temperature into a column density of hydrogen (Irvine et al. 1987) by assuming that the CS(2–1) line is optically thin, that a single Boltzmann temperature characterizes the level populations, and a fractional abundance derived by Bujarrabal et al. (1988), $[CS]/[H_2] \sim 4 \times 10^{-8}$. Carbon monosulfide is a high-density

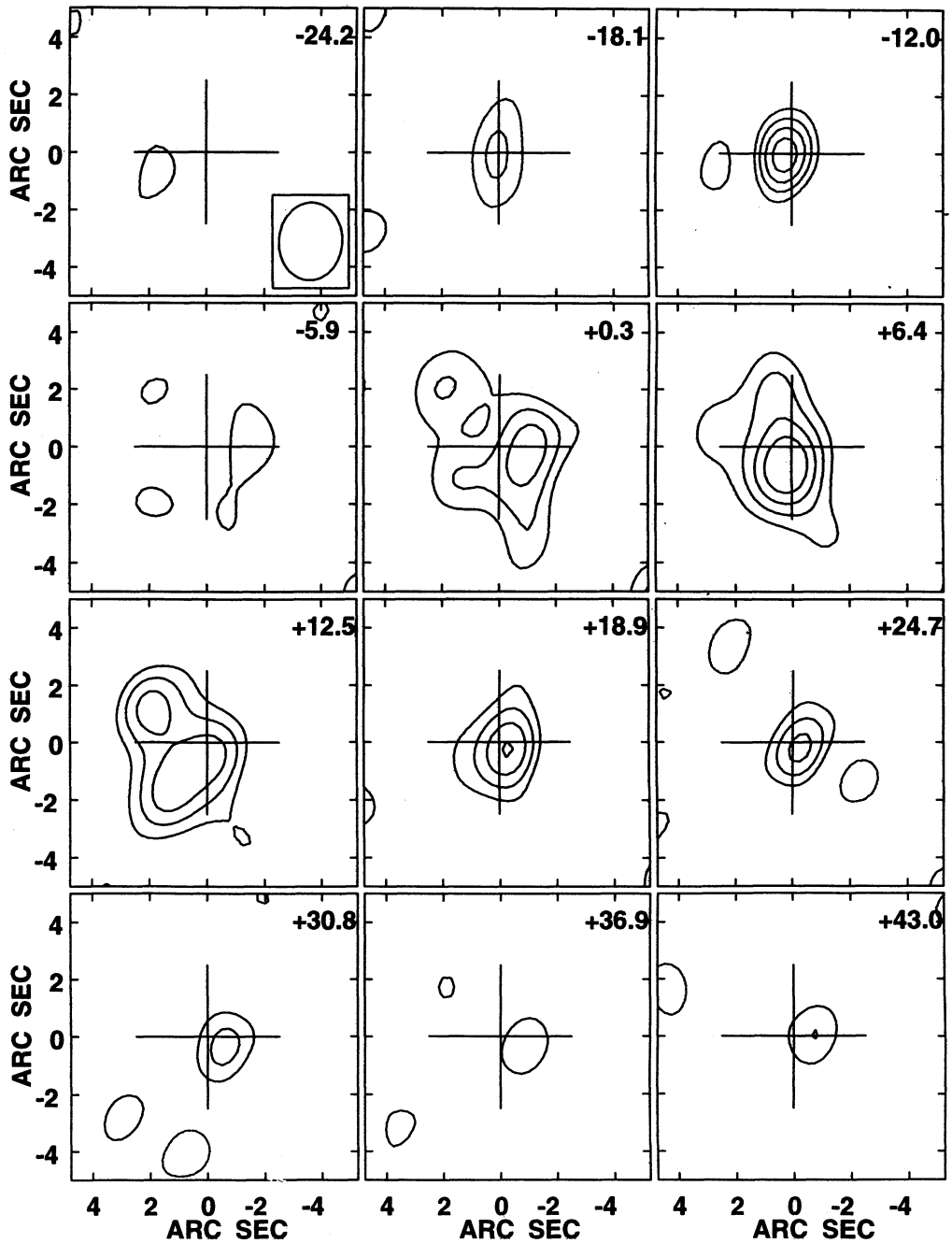

FIG. 1.—The channel maps for the CS(2–1) line emission. The spectral resolution is 6.12 km s^{-1} channel^{-1}. The velocities listed in the map are the channel central velocity with respect to the systemic velocity of -21.5 km s^{-1}. The continuum flux of 1.43 Jy has been subtracted. Note the intense absorption for the channels at -18.1 and -12.0 km s^{-1}. The synthesized beam is shown in the lower right-hand corner of the upper left-hand panel. The 1 σ level is at 0.045 Jy beam^{-1}, and the contour levels are at -0.09, 0.09, 0.135, 0.180, and 0.225 Jy beam^{-1}.

tracer: for $T = 100$ K, $n_{\rm crit} = 4.4 \times 10^5$ cm^{-3}. Assuming a temperature of 200 K for the CS gas yields a column density of $\sim 3 \times 10^{23}$ cm^{-2} and a total H_2 mass of order 2 $M_\odot$. With information regarding only one transition, the uncertainty in the final order-of-magnitude mass determination is large, primarily due to the lack of temperature information in the emitting gas. We can better constrain the physical conditions by considering the CS(3–2) transition observed by Bujarrabal et al. (1988). Correcting for the differences in the telescope beams, we compute the ratio:

$$R = \frac{T_{2-1}}{T_{3-2}} \lesssim 0.129 .$$

A consequence of using interferometric data is that an unknown amount of flux is resolved out, and we have thus used an inequality in the above equation to reflect our underestimate of the CS(2–1) line flux. We utilized the large velocity

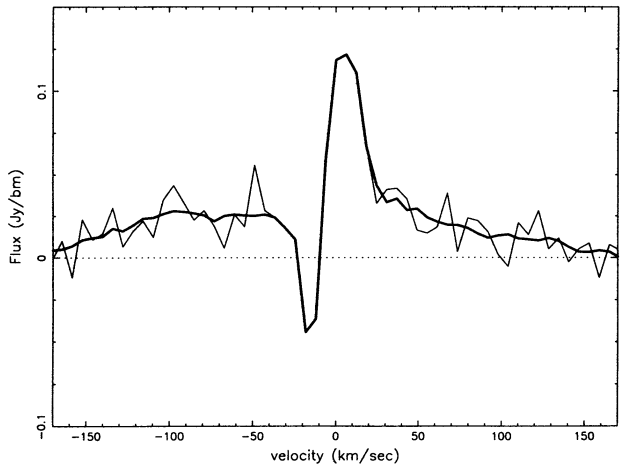

FIG. 2.—The average spectrum over the central 5″ (about 3.7 beam areas) of the CS(2–1) line data. The absorption feature is not well-resolved. The peak flux in the spectrum is at 0.115 ± 0.013 Jy beam^{-1} (2.35 ± 0.23 K). The dark line represents a heavily smoothed version of the spectrum.

gradient (LVG) model (Cantor 1970) with a grid of values for the density and temperature of the CS gas. The best match between the observed and predicted line ratios required a high temperature ($T_{\rm kin} \sim 500$ K) and densities near 6×10^5 cm^{-3}. However, while the computed density seems reasonable, the temperature we have derived is not. The CS(2–1) rotational transition is at 2.4 K and the CS(3–2) at 4.72 K: these lines are very poor temperature probes for hot gas. The LVG code computes only level populations with a model of the first 11 levels: even the $J = (11–10)$ line is at 26 K. We thus conclude only that the CS gas has a temperature $\gtrsim$50–100 K. If we assume that the CS gas is arranged in a uniform sphere of constant density and use the CS abundance determined by Bujarrabal et al. (1988), we can determine the total molecular mass surrounding CRL 618. We chose an angular radius equal to $r = 2 \sum_i F_i/\pi F_M$, where F_i is the flux of the ith pixel, and F_M is the maximum flux in the map. For the purposes of this analysis, we considered pixels within 5″ of the phase center. Our CS(2–1) map gives $r_{\rm sphere} = 2\farcs6$ and a total envelope H_2 mass of $1.0 \pm 0.2\ M_\odot$. Due to the missing flux in these maps, however, the density and corresponding mass are lower limits. The large molecular mass that we have detected is consistent with CRL 618's designation as a protoplanetary nebula (Westbrook et al. 1975) and is confirmed by single-dish observations of other molecules (Bujarrabal et al. 1988).

We can also explore the CS in the outer envelope, where the gas is too tenuous to emit efficiently. Given the optical depth in the absorption feature and assuming the same abundance as above, we estimate a total molecular column density of $\sim 5 \times 10^{20}$ cm^{-2}. We cannot say more about the gas responsible for the absorption without additional spectra at other frequencies as well as higher angular resolution to determine the extent of the absorbing material.

It is currently believed that the molecular configuration of CRL 618 is the result of the interaction between shock-excited molecules in the collimated, fast wind from the central star and a preexisting, cool molecular halo (Martin-Pintado & Bachiller 1992; Young et al. 1991; Gammie et al. 1989). High-speed outflows, with line-shapes similar to those in this paper but in the molecules of CO (Gammie et al. 1989), NH_3 (Martin-Pintado & Bachiller 1992), HC_3N, and HCO^+ (Cernicharo et al. 1989) have been seen from CRL 618, suggesting a generation mechanism common to all molecular material in its shell. Dynamical arguments also support this scenario. Assuming a distance of 1.5 kpc (Lo & Bechis 1976) to CRL 618, a 3″ outflow moving at the constant speed of 20 km s^{-1} requires $\sim$500 yr to occupy the CS emission region. Since the optical and radio brightening timescales are much shorter, it is possible that the assumption constant velocity motion is not applicable. The dynamical timescale for the CS outflow can be significantly shortened if either the CS gas or the atomic gas which condensed into CS molecules were ejected at a much higher velocity and then shocked. This would result in a smaller observed velocity and collisionally excited molecular emission. Our CS maps show elongation in the northwest–southwest and northeast–southwest directions: these extensions may be high-velocity gas streaming out of holes in the cool halo or high-velocity jets flowing from the core. HCN line maps at high angular resolution (2″.4 × 3″.4) by Neri et al. (1992) have been interpreted in a similar manner. The nature of the collimating process is unknown, but many planetary nebulae are characterized by a density enhancement along the equator, and in some cases, a spherically symmetric wind unleashed from the central star can interact with this density distribution to result in a bipolar outflow (Mellema 1993; Icke; Icke, Balick, & Frank 1992). In a forthcoming paper, we discuss observations of the CO (1–0) line which is a useful probe of the lower density environment surrounding the CS core (Hajian, Phillips, & Terzian 1994).

CRL 618 shows hot NH_3 gas with $T = 270$ K (Martin-Pintado & Bachiller 1992) and hot HCN gas with $T \geq 400$ K (Neri et al. 1992). Our CS observations demonstrate the presence of CS gas consistent with the high-temperature limit of our observed transitions ($T \gtrsim 100$ K). Given the small ratio of turbulent energy content to bulk energy of the outflow (about 10%), we conclude that the dispersion in the CS shell is slow, and the expansion of the shell can be approximated by a single expansion velocity.

4. SUMMARY AND CONCLUSIONS

We have mapped, for the first time, the CS(2–1) line and the λ3.1 mm continuum from the protoplanetary nebula CRL 618 with high angular resolution. We summarize our major conclusions below.

1. The continuum source is pointlike ($\theta \lesssim 2\farcs5$) with a flux of 1.43 Jy at λ3.1 mm.
2. The CS envelope has a double bipolar morphology, with one axis oriented almost at right angles to the other axis.
3. The spectral profile of the CS line is dominated by a P Cygni feature with emission wings out to $\approx +20$ km s^{-1} and an absorption feature between approximately -20 and -5 km s^{-1}. This narrow line component sits atop low-intensity CS emission wings which extend across $\geq$340 km s^{-1}. The total integrated line flux in the emission line after interpolating over the absorption feature is 28.52 Jy km s^{-1}. Based on the narrow width of the absorption feature, the turbulent energy content in the cool CS halo is small, amounting to only $\sim$10% of the bulk kinetic energy. This implies the halo is smoothly expanding at a constant (in position) velocity.
4. By incorporating our CS(2–1) observations and the single-dish CS(3–2) data from Bujarrabal et al. (1988), we have estimated the physical conditions in the CS gas using the LVG code. We find the emitting CS gas is in the high-temperature

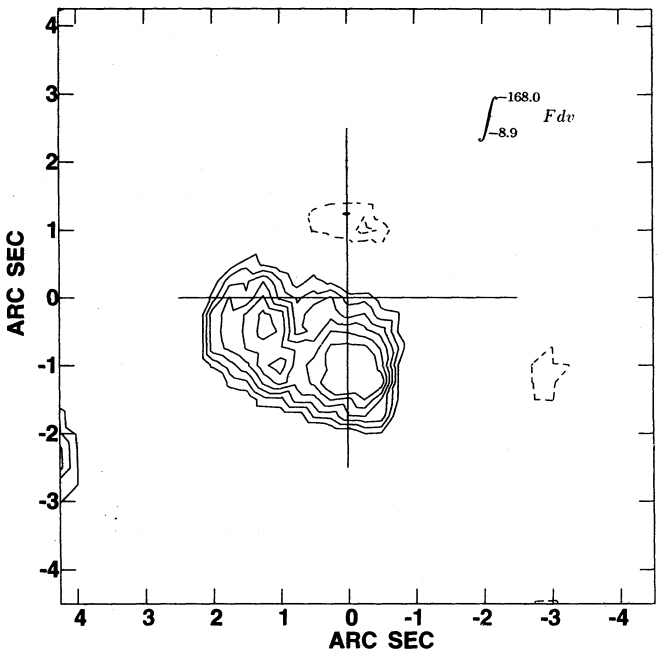

FIG. 3*a*

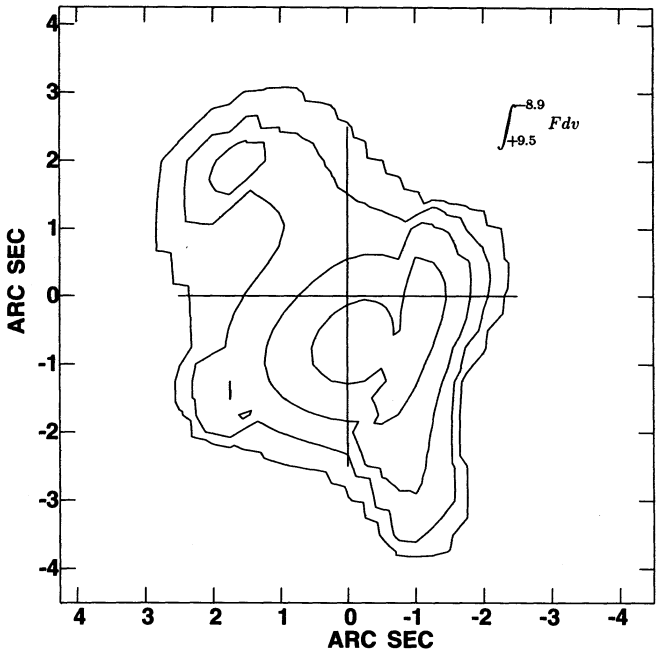

FIG. 3*b*

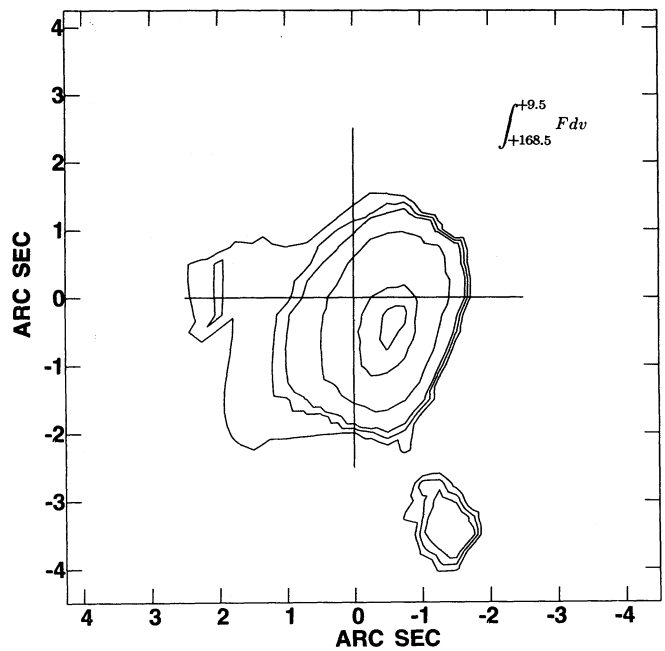

FIG. 3*c*

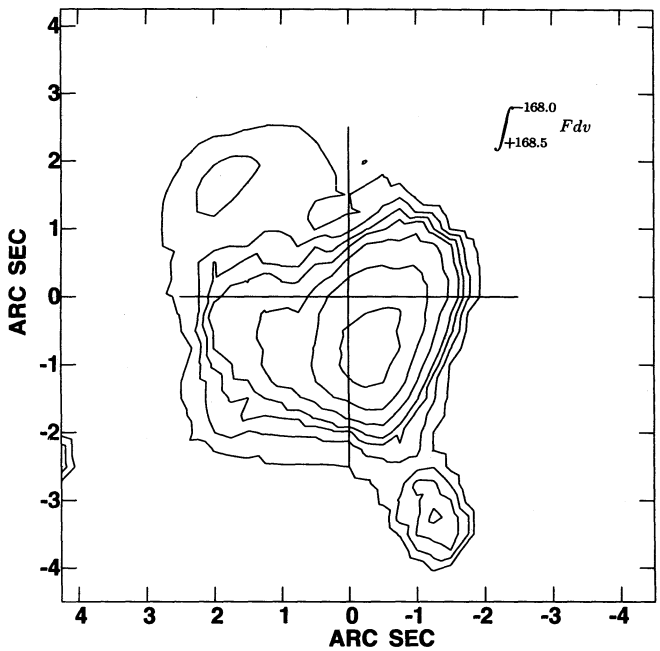

FIG. 3*d*

FIG. 3.—The blueshifted, high-velocity CS emission from CRL 618. This map has been integrated from -168.0 to -8.9 km s^{-1}, and the contour levels are at -1.5, -1.0, 1.0, 1.5, 2.0, 2.5, 3.0, and 3.5 Jy beam^{-1} km s^{-1}. The cross represents the position of the H II region. Note the absorption north of the map center. (*b*) The unshifted, low-velocity CS emission from CRL 618. This map has been integrated from -8.9 to $+9.5$ km s^{-1}, and the contour levels are at 1.0, 1.5, 2.0, and 2.5 Jy beam^{-1} km s^{-1}. The cross represents the position of the H II region. (*c*) The redshifted, high-velocity CS emission from CRL 618. This map has been integrated from $+9.5$ to $+168.5$ km s^{-1}, and the contour levels are at 1.5, 2.0, 2.5, 5.0, 10.0, and 11.5 Jy beam^{-1} km s^{-1}. This emission is shifted in position relative to Fig. 3*a*. (*d*) The total integrated CS emission from -168.0 to $+168.5$ km s^{-1}. The contour levels are 2.0, 3.0, 4.0, 5.0, 7.0, 10.0, 15.0, and 20.0 Jy beam^{-1} km s^{-1}.

limit of the transitions ($T \gtrsim 50$–100 K) and has a density of $\gtrsim 10^{5.8}$ cm^{-3}. These values imply a total nebular mass of $\gtrsim 1$ $M_\odot$ with an uncertainty of $\sim 20\%$. Due to the wide range of high velocities present in the outflow, it is likely that the high-velocity CS emission is shock-excited. A large decleration in a rapid outflow would help to explain the long dynamical timescales if constant motion at ≈ 20 km s^{-1} is assumed. The shocked CS is probably the result of the interaction of the quickly expanding, emitting CS outflow with a slowly expanding, dense, cool, and absorbing CS halo. We approximate the column density of the low-velocity, cool envelope gas to be $\sim 5 \times 10^{20}$ cm^{-2} from the absorption feature in the CS spectrum.

We would like to thank G. Stacey for several useful discussions and P. Goldsmith for his help with the calculations

and his generous contribution of the LVG FORTRAN code. A. H. and Y. T. were supported in part by the National Astronomy and Ionosphere Center which is operated by Cornell University under a cooperative agreement with the National Science Foundation. The OVRO millimeter interferometer is supported by NSF grant AST 90-16404.

REFERENCES

Bachiller, R., Gomez-Gonzalez, J., Bujarrabal, V., & Martin-Pintado, J. 1988, A&A, 196, L5
Bujuarrabal, V., Gomez-Gonzalez, J., Bachiller, R., & Martin-Pintado, J. 1988, A&A, 204, 242
Cantor, I. J. 1970, MNRAS, 149, 111
Carsenty, U., & Solf, J. 1982, A&A, 106, 307
Cernicharo, J., Guelin, M., Martin-Pintado, J., Penalver, J., & Mauersberger, R. 1989, A&A, 222, L1
Deguichi, S., Claussen, M. J., & Goldsmith, P. F. 1986, ApJ, 303, 810
Gammie, C. F., Knapp, G. R., Young, K., Phillips, T. G., & Falgarone, E. 1989, ApJ, 345, L87
Gottlieb, E. W., & Liller, W. 1976, ApJ, 207, L135
Icke, V., Balick, B., & Frank, A. 1992, A&A, 253, 224
Hajian, A. R., Phillips, J. A., & Terzian, Y. 1994, in preparation
Irvine, W. M., Goldsmith, P. F., & Hjalmarson, A. in Interstellar Processes, ed. D. J. Hollenbach & H. A. Thronson, Jr. (Dordrecht: Reidel), 561
Kelly, D. M., Latter, W. B., & Rieke, G. H. 1992, ApJ, 395, 174
Kleinmann, S. G., Sargent, D. G., Moseley, H., Harper, D. A., Loewenstein, R. F., Telesco, C. M., & Thronson, H. A. 1978, A&A, 65, 139
Knapp, G. R., Sandell, G., & Robson, E. I. 1993, ApJS, 88, 173
Kwok, S. 1986, in Late Stages of Stellar Evolution. Proc. Workshop in Calgary (Dordrecht: Reidel)
Kwok, S., & Bignell, R. C. 1984, ApJ, 276, 544
Kwok, S., & Feldman, P. A. 1981, ApJ, 267, L67
Kwok, S., Hrivnak, B. J., & Milone, E. 1986, ApJ, 303, 451
Lo, K. Y., & Bechis, K. 1976, ApJ, 205, L21
Martin-Pintado, J., & Bachiller, R. 1992, ApJ, 391, L93
Mellema, G. 1993, Ph.D. thesis, Univ. Leiden
Neri, R., Garcia-Burillo, S., Guelin, M., Cernicharo, J., Guilloteau, S., & Lucas, R. 1992, A&A, 262, 544
Padin, S., et al. 1993, IEEE Instr., 42, 793
Schmidt, G. D., & Cohen, M. 1981, ApJ, 246, 444
Scoville, N. Z., Carlstrom, J. E., Chandler, C. J., Phillips, J. A., Scott, S. L., Tilanus, R. P. J., & Wang, Z. 1993, PASP, 105, 1482
Shibata, K. M., Deguchi, S., Hirano, N., Kameya, O., & Tamura, S. 1994, ApJ, 415, 708
Soptka, R. J., Hildebrand, R., Jaffe, D. T., Gatley, I., Roellig, T., Werner, M., Jura, M., & Zuckerman, B. 1985, ApJ, 294, 242
Trammell, S. R., Dinerstein, H. L., & Goodrich, R. W. 1993, ApJ, 402, 249
Westbrook, W. E., Becklin, E. E., Merrill, K. M., Neugebauer, G., Schmidt, M., Weillner, S. P., & Wynn-Williams, C. G. 1975, ApJ, 202, 407
Yamamura, I., Shibata, K. M., Kasuga, T., & Deguichi, S. 1994, ApJ, 427, 406
Young, K., Serabyn, G., Phillips, T. G., Knapp, G. R., Gusten, R., & Schulz, A. 1992, ApJ, 385, 265